928-80 Can Electrocardiogram Help to Differentiate Emery-Dreifuss Muscular Dystrophy from Other Muscular Dystrophies?

Julien Bensaid, Jean Michel Vallat, Patrice Virot. *Departments of Cardiology and Neurology, Dupuytren Hospital, Limoges, France*

Emery-Dreifuss muscular dystrophy (EDMD) is a rare X-linked muscular disease with a potentially lethal cardiac arrhythmia.

The purpose of this study was to determine if electrocardiogram (ECG) was useful to differentiate EDMD from other muscular dystrophies, mainly facioscapulohumeral dystrophy and limb-girdle muscular dystrophy that usually have a benign course and a good prognosis.

Our own experience consists of 3 patients of the same family with EDMD, 2 of them having a persistent atrial standstill during 22 years follow-up. Therefore we have reviewed the ECG patterns of 125 cases of EDMD reported in the literature and found persistent atrial standstill (PAS) in 37 patients (30%) and complete (31 patients, 25%) or incomplete (22 patients, 18%) A-V block.

On the contrary no case of atrial standstill was recorded in the patients with the diagnoses of facioscapulohumeral dystrophy or other types of muscular dystrophies based on rigorous clinical criteria.

On an other hand, in a survey of the etiologies of 109 cases of PAS, we have found 36 patients with EDMD (33%). Moreover in 27 patients with EDMD who had a 12 lead surface ECG, PAS was associated with a left anterior fascicular block (LAFB) in 14 cases (52%). Conversely in 51 patients without EDMD, PAS was associated with a LAFB in 5 cases only (10%, $p < 0.01$).

Conclusion. 1 The presence of persistent atrial standstill can probably help to differentiate Emery-Dreifuss muscular dystrophy from other muscular dystrophies more especially as a left anterior fascicular block is associated.

2 Pacemaker insertion is recommended in that case to avoid the risk of sudden death.

928-81 Importance of Holter Monitoring, as Compared to Exercise Testing, in Revealing ST-segment Changes in Patients with Syndrome X

Gaetano A. Lanza, Alessandro Manzoli, Giuseppe Colonna, Vincenzo Pasceri, Giuseppe M.C. Rosano, Filippo Crea, Attilio Maseri. *Istituto di Cardiologia, Università Cattolica del S. Cuore, Roma, Italy*

Despite growing interest and a large body of studies on syndrome X (anginal chest pain and angiographically normal coronary arteries), there are no data concerning the respective diagnostic value of exercise testing (ExT) and ambulatory Holter monitoring (HM) in revealing ischemic ST-segment changes in these patients. To address this problem, we performed ExT and 24-hour HM, off therapy, in 38 syndrome X patients (27 women, age 54 ± 8 years). ExT showed ST-segment depression (STd) in 28 patients (74% Group 1), whereas it was normal in 10 patients (26%, Group 2). Anginal chest pain during ExT was reported by 10 patients (36%) of Group 1 and 9 patients (90%) of Group 2 ($p < 0.01$). On the other hand, STd episodes were detected on HM in 22 patients (59%), 17 (61%) of whom belonging to Group 1 and 5 (50%) to Group 2 (p = NS). On the whole, 129 STd episodes, 14 (11%) of which associated to anginal pain, were found in the 22 patients (mean 5.8 ± 4.6 episodes/patient). A total of 21 STd episodes (5 associated to anginal pain) were detected on HM in the 5 patients with negative ExT (mean 4.3 ± 3.5 episodes/patient, range 1–10). In these 5 patients, heart rate at 1 mm STd during HM was significantly lower than that achieved at peak exercise during ExT (111 ± 19 vs. 136 ± 22 bpm, $p = 0.01$). The prevalence of positive HM in patients with negative ExT in our syndrome X patients was significantly higher than that observed in an unselected group of 76 patients with stable angina, significant coronary artery disease and negative ExT (50% vs 8%, $p < 0.01$). Thus, our data show that HM, with respect to ExT, has a significant additional diagnostic value in revealing the occurrence of ischemic ST-segment changes in patients with syndrome X. These findings also support the hypothesis that a microvascular vasoconstriction, rather than an impaired vasodilation, plays a major role in the pathophysiologic mechanisms leading to transient ischemia in these patients.

928-82 Neural Sprouting and Ventricular Tachycardia

Peng-Sheng Chen, Lan S. Chen, Paul L. Wolf, Michael C. Fishbein. *Cedars-Sinai and Childrens Medical Centers, Los Angeles, VA; UCSD Medical Centers, San Diego, California*

Damaging the axons of a nerve may result in initial degeneration of the distal axon, followed by a regenerative process which forms aberrant synapses (neural sprouting). Because myocardial infarction (MI) can result in cardiac nerve damage, neural sprouting will follow, and could contribute to the generation of ventricular tachycardia (VT). To test this hypothesis, we retrospectively studied 7 pts with drug-resistant sustained monomorphic VT who underwent surgical subendocardial ablation. The age ranged from 54 to 77 years. All pts had a history of MI. Five pts had discrete ventricular aneurysm and 2 pts had a history of sudden cardiac death. Computerized mapping was used to determine the VT origin. Surgical treatment was performed by endocardial excision techniques. Paraffin-embedded tissue samples from the sites where VT were originated were sectioned and stained with Hematoxylin and Eosin (H & E), and for S-100 protein using standard immunohistochemical techniques to identify Schwann cells. The results of S-100 protein stain were classified on a scale of 0 to 4+ based on light microscope examination, with 0 being negative and 4+ being strongly positive. The H & E stain showed various degrees of fibrosis in all specimens, compatible with old MI. The S-100 protein stain was positive in 6 of 7 pts, showing numerous small regenerated nerve twigs within the region of MI not seen in normal myocardium. The average strength of S-100 protein stain was 1.7 ± 1.0+ (range 0+ to 3+). Tyrosine hydroxylase stain was performed in 2 pts. Both showed positive staining. We conclude that sympathetic neural sprouting is present at the origin of VT and may play a role in the generation of VT and sudden death after MI.

929 Assessment of Myocardial Perfusion and Function by MR

Monday, March 20, 1995, 3:00 p.m.–5:00 p.m.
Ernest N. Morial Convention Center, Hall E
Presentation Hour: 3:00 p.m.–4:00 p.m.

929-61 Contrast Wash-in During MRI Myocardial Perfusion Imaging in Patients with Q-Wave Myocardial Infarction

Mark A. Lawson, H. Ross Singleton, Edward G. Walsh, Mark Doyle, Maryann Roney, Gerald G. Blackwell, Gerald M. Pohost. *University of Alabama at Birmingham, Birmingham, AL*

Eleven patients (7 anterior and 4 inferior) with Q-wave myocardial infarction (QMI) undergoing radionuclide imaging were studied using MR perfusion imaging techniques and quantitative computer analysis of the signal intensity (SI)-time curves. The purpose of this study was to determine the relative accuracy of slope (wash-in) and peak SI when compared to radionuclide images in myocardial regions with corresponding Q-waves on the electrocardiogram.

Patients underwent MR perfusion imaging using an ultrafast interpolated keyhole acquisition during bolus administration of gadoteridol (0.1 mmol/kg). Perfusion images were obtained under resting conditions and after dipyridamole (0.56 mg/kg). Radionuclide images were obtained the same day by either thallium exercise testing or hybrid thallium-^{99m} Tc sestamibi rest-dipyridamole stress testing and available for comparison. The slope of the SI-time curve (regression analysis) and peak SI were compared between normal and infarcted myocardium. The slope and SI were normalized to left ventricular cavity values, averaged, and compared using t-test statistical analysis.

Eight QMI patients with scarred myocardium determined by the radionuclide study had decreased slope (0.14 vs 0.47, $p < 0.001$) and peak SI (0.38 vs 0.58, $p = 0.01$) compared to normal regions. Slope (0.14 vs 0.23) and SI (0.38 vs 0.46) increased in the scarred regions following dipyridamole but not significantly. Normal regions had increased slope (0.47 vs 0.66, $p = 0.02$) but not SI following dipyridamole. Three QMI patients had reversible ischemia in Q-wave regions. Slopes were higher when compared to patients with scar (0.39 vs 0.14, $p = 0.02$) and more closely approximated normal regions (0.39 vs 0.55, p = NS). Ischemic regions had no significant change in slope (0.39 vs 0.40) or SI (0.54 vs 0.50) following dipyridamole.

These data suggest that slope may be a stronger indicator of artery patency and closely parallels the results of radionuclide imaging.

929-62 Altered Myocardial High-Energy Phosphate Metabolism in Aortic Valve Disease: Failing Myocardium or Inadequate Blood Supply?

Josef Kautzner, Ales Linhart, Dana Kurkova [1], Vit Herynek [1], Milan Hajek. *Charles' University Medical School I, Prague, Czech Republic; [1] Institute for Clinical and Experimental Medicine, Prague, Czech Republic*

31P MR spectroscopy has become a valuable tool for assessment of alterations in myocardial high-energy phosphate (HEP) metabolism in vivo. In this respect, depression of the phosphocreatine (Pcr) to ATP ratio has been suggested as an early marker of heart failure. This may be of clinical relevance during natural history of aortic regurgitation. To address this issue, 31P MR spectroscopy (ECG triggered 1D ISIS technique with correction for blood contamination) was performed preoperatively in 9 male patients (Group I, mean age 53.7 ± 10.3 years) with aortic stenosis (mean aortic valve gradient 58.1 mmHg), 9 male patients (Group II, mean age 45.1 ± 9.5 years) with aortic regurgitation, and in 12 age and sex matched healthy volunteers. All patients underwent right and left heart catheterization, left ventricular and coronary angiography, and routine echocardiography.

No significant differences in baseline hemodynamic parameters (including LV ejection fraction) were found between group I and II except for systolic aortic pressure (102 ± 12.3 vs 143.1 ± 27.7 mmHg, $p < 0.002$), pulse pressure (39.1 ± 12.5 vs 88.1 ± 21.9 mmHg, $p < 0.000$), LV volume (LV end-diastolic volume index 85.4 ± 29.7 vs 141.1 ± 29.4 ml/m^2, $p < 0.001$) and aortic valve gradient. PCr/ATP ratios were as follows:

Group	PCr/γ ATP	PCr/α ATP	PCr/β ATP
I	2.28 ± 2.09	0.78 ± 0.62*	1.01 ± 0.62*
II	2.80 ± 1.75	1.34 ± 0.60*	1.59 ± 0.49*
III	2.98 ± 1.78	1.74 ± 0.51*	2.01 ± 0.30*

*$p < 0.05$

Positive correlation was revealed between Pcr/α ATP or Pcr/β ATP and systolic aortic pressure ($r = 0.60$, $p < 0.014$ and 0.009, respectively) as well as pulse pressure ($r = 0.50$, $p < 0.036$ and $r = 0.53$, $p < 0.023$, respectively) in all patients.

In conclusion, detection of significant impairment of HEP metabolism in aortic stenosis only and relationship of these changes to aortic, and therefore to coronary perfusion pressure appear to reflect imbalance in myocardial oxygen/supply ratio rather than deterioration of LV function itself.

929-63 Dobutamine Stress Cine Magnetic Resonance Imaging versus PET for Detection of Myocardial Viability

Valérie Julien, Michel Ovize, Marc Janier, Claire Baldy, Sameh Bakhoum, Roland Itti, Didier Revel, Xavier André-Fouët. *Hopital Cardiologique and CERMEP, Lyon, France*

To identify viable myocardium before coronary revascularization, we prospectively submitted eleven patients (60 ± 7 yrs; 11 M) with previous Q-wave myocardial infarction to ^{18}FDG-Positon Emission Tomography and low-dose (5 to 10 μg/kg/min) dobutamine cine-MRI. ^{18}FDG uptake >60% was considered indicative of viable tissue. Quantitation of systolic wall thickening/thinning (SW) was performed by use of a computer software allowing automatic detection of epicardial and endocardial outlines, at rest and under 5, 7.5 and 10 μg/kg/min of dobutamine. Heart slices of both ^{18}FDG-PET scans and dobutamine cine-MRI were divided in 8 segments, matched and analyzed by observers blinded to clinical data. Sixty-five segments were considered viable by ^{18}FDG-PET; in this subgroup, rest SW thickening averaged 47 ± 5% and improved by 43 ± 8% under low-dose dobutamine. In the remaining 23 segments considered non viable by PET, rest SW thickening averaged 14 ± 7%* (*$p < 0.05$ vs viable segment group) and further worsened by −13 ± 8%* during low-dose dobutamine stress (*$p < 0.05$ versus viable segment group). Positive predictive value of low-dose dobutamine stress cine-MRI for assessment of myocardial viability was 84%. These data suggest that quantitative assessment of regional wall motion by dobutamine cine-MRI may help discriminate viable from non viable myocardium as defined by ^{18}FDG-Positon Emission Tomography.

929-64 Global Cardiac Function Using Active Contour Models with Fast Breath-hold MRI

Daniel C. Bloomgarden, Zahi A. Fayad, Cheng-Ning Chang, Victor A. Ferrari, Alistair A. Young [1], Leon Axel. *University of Pennsylvania, Philadelphia, PA; [1] University of Auckland, Auckland, New Zealand*

Fast MR imaging techniques now permit rapid acquisition of gated cardiac images spanning the entire ventricle through most of the cardiac cycle. Quantitative global function analysis requires extraction of the myocardial borders in the images. However, manual analysis is tedious and time consuming while fully automated techniques are limited because of image artifacts and poor blood/myocardial contrast in certain regions, especially with fast-imaging techniques. We have developed a fast, interactive, semi-automated method for defining the myocardial borders. We present the initial results of this method using MR images of static phantoms, dog hearts, and normal volunteers.

Ten healthy adult volunteers (ages 18–34) were imaged with a clinical 1.5 Tesla MRI system (GE) using a fast gradient-echo ECG-gated pulse sequence which acquired 8–12 cardiac phases from end-diastole (ED) past end-systole during a breath-hold. 12–15 short-axis (SA) images were acquired from the pulmonary valve to the LV apex. The imaging parameters were: FOV = 24–26 cm, flip angle = 33°, slice thickness = 6 mm, slice spacing = 2 mm, TR/TE = 7.2/2.6 msec.

Analysis was done with our customized software (SPAMMVU) using our contour tracking routine. This method models each contour as an analytic function (with an associated effective strain "energy") that is attracted to edges in the image, but can be manipulated by the user to outline regions with poor contrast or to avoid artifacts. Internal stiffness of the model results in smoothing and fast outlining. Typical analysis takes less than 20 minutes vs. 1–2 hours for a manual method.

Volumes were computed using Simpson's rule. Measured volumes of static phantoms had less than 5% error compared to truth. Errors in calculated LV mass of dog hearts by MRI were less than 10% compared with actual *ex vivo* weight. LV mass of normal volunteers was determined at ED and ES. Linear regression analysis of ED LV mass vs. ES LV mass yields an excellent correlation (R^2 of 0.94). A similar analysis of LV stroke volume (SV) vs RV SV yields an R^2 value of 0.85.

Our semi-automated contour extraction program provides a fast, reproducible, and accurate method for quantifying cardiac global function from MR images.

929-65 Mechanisms of Hyperenhancement by Contrast Enhanced Magnetic Resonance Imaging are Related to Injured Myocardial Mass in Patients with Acute Myocardial Infarction

Joao A.C. Lima, Gabriel Nazareno, Robert Judd, Carlos Lugo-Olivieri, Cynthia Siu, Elias A. Zerhouni. *Johns Hopkins Hospital, Baltimore, MD*

The extent of injured myocardium is directly related to infarct size after acute myocardial infarction (AMI). Myocardial hyperenhancement during ultrafast contrast enhanced magnetic resonance imaging (CEMRI) reflects ischemic injury and its mechanism; extracellular volume expansion with or without washout impairment may be related to the magnitude of ischemic injury; edema formation with or without cell death. To investigate the relationship between the extent of myocardial injury and the mechanism of myocardial hyperenhancement by CEMRI we studied 19 patients after AMI. Spoiled GRASS, TR = 6.5 ms, TE = 2.3 ms, 4 short-axis images were analyzed, and the ratio of signal intensity in myocardium to blood from injured (IN) and normal (NL) regions was obtained at 50 secs, 160 secs and 600 secs. after I.V. contrast (gadoteridol 0.1 mmol/kg). Percent injured myocardial mass was calculated as the ratio of hyperenhanced myocardium to total LV mass by planimetry. Patients were divided into two groups according to the mechanism of signal hyperenhancement. Group 1 (N = 9) was defined by a parallel upwards displacement (ANOVA $p < 0.002$) of the injured myocardium/blood ratio over time relative to normal myocardium consistent with pure extracellular expansion. Group 2 (N = 11) had upwards displacement (ANOVA $p < 0.001$) with significant slope (ANOVA $p < 0.001$) consistent with impaired washout (see Figure). Injured mass was greater in Group 2 (31.9 ± 6.4%) than in Group 1 (15.9 ± 5.0%, $p < 0.001$).

In conclusion, the mechanism of myocardial hyperenhancement is related to the extent of ischemic injury after AMI, with greater injury associated with the presence of washout impairment, suggesting cell death. These relationships may be explored to assess myocardial viability after AMI by CEMRI.

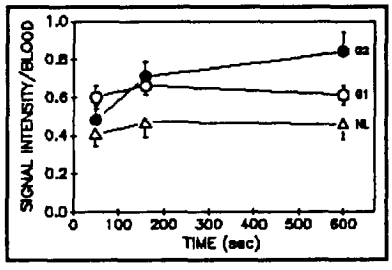

929-66 Validation of a New Method for Calculating Continuous Transmural Distributions of Strain in the Ventricles Using Magnetic Resonance Tagging

Michael J. Moulton, Lawrence L. Creswell, Stephen W. Downing, Barna A. Szabó, Michael W. Vannier, Michael K. Pasque. *Washington University, St. Louis, Missouri*

Magnetic resonance imaging (MRI) tagging provides information about deformation at many intramural points in the ventricular wall and thus offers the potential to characterize the transmural pattern of deformation. We have developed a method to calculate continuous transmural distributions of finite strains across the ventricular wall from the deformation of the MR "tag lines". The purpose of this study was to quantify the error in this technique by comparing strains computed with our method to a "gold standard" solution. Seven dogs underwent cine MRI with tagging, generating dark grid patterns of presaturations on the images. Deforming tag lines were tracked using an automated algorithm. A parametric representation of tag line deformation was developed. Strains were calculated in a local region bounded by five to six tag lines by constructing a local mapping from the region on the undeformed image to the same region on the deformed image. The mapping was defined by fitting a polynomial "surface" to the measured deformations of the tag lines and by employing a smoothing term to control the trade-off between fidelity of the data and surface and the smoothness of the